Invest New Drugs (2016) 34:300–318
DOI 10.1007/s10637-016-0342-y

PHASE I STUDIES

Metabolite profiling of the multiple tyrosine kinase inhibitor lenvatinib: a cross-species comparison

Anne-Charlotte Dubbelman[1,2,7] · Cynthia M. Nijenhuis[2] · Robert S. Jansen[2] · Hilde Rosing[2] · Hitoshi Mizuo[3] · Shinki Kawaguchi[3] · David Critchley[4] · Robert Shumaker[5] · Jan H. M. Schellens[1,6] · Jos H. Beijnen[2,6]

Received: 10 February 2016 / Accepted: 7 March 2016 / Published online: 28 March 2016

Summary Lenvatinib is an oral, multiple receptor tyrosine kinase inhibitor. Preclinical drug metabolism studies showed unique metabolic pathways for lenvatinib in monkeys and rats. A human mass balance study demonstrated that lenvatinib related material is mainly excreted via feces with a small fraction as unchanged parent drug, but little is reported about its metabolic fate. The objective of the current study was to further elucidate the metabolic pathways of lenvatinib in humans and to compare these results to the metabolism in rats and monkeys. To this end, we used plasma, urine and feces collected in a human mass balance study after a single 24 mg (100 μCi) oral dose of ^{14}C-lenvatinib. Metabolites of ^{14}C-lenvatinib were identified using liquid chromatography (high resolution) mass spectrometry with off-line radioactivity detection. Close to 50 lenvatinib-related compounds were detected. In humans, unchanged lenvatinib accounted for 97 % of the radioactivity in plasma, and comprised 0.38 and 2.5 % of the administered dose excreted in urine and feces, respectively. The primary biotransformation pathways of lenvatinib were hydrolysis, oxidation and hydroxylation, N-oxidation, dealkylation and glucuronidation. Various combinations of these conversions with modifications, including hydrolysis, gluthathione/cysteine conjugation, intramolecular rearrangement and dimerization, were observed. Some metabolites seem to be unique to the investigated species (human, rat, monkey). Because all lenvatinib metabolites in human plasma were at very low levels compared to lenvatinib, only lenvatinib is expected to contribute to the pharmacological effects in humans.

This work was financially supported by Eisai Co. Ltd.

Anne-Charlotte Dubbelman and Cynthia M. Nijenhuis are co-first authors.

Electronic supplementary material The online version of this article (doi:10.1007/s10637-016-0342-y) contains supplementary material, which is available to authorized users.

✉ Anne-Charlotte Dubbelman
a.c.dubbelman@gmail.com

✉ Cynthia M. Nijenhuis
cynthia.nijenhuis@slz.nl

[1] The Netherlands Cancer Institute, Division of Clinical Pharmacology, Department of Medical Oncology, Amsterdam, The Netherlands

[2] Antoni van Leeuwenhoek / The Netherlands Cancer Institute and MC Slotervaart, Department of Pharmacy & Pharmacology, Louwesweg 6, 1066 CE Amsterdam, The Netherlands

[3] Eisai Co. Ltd., Drug metabolism and Pharmacokinetics Japan, Tsukuba, Japan

[4] Eisai Ltd., Chief Clinical Officer Department, Clinical Pharmacology, Hatfield, UK

[5] Eisai Inc., Oncology Product Creation Unit, Clinical Pharmacology and Translational Medicine, Woodcliff Lake, NJ, USA

[6] Division of Pharmacoepidemiology and Clinical Pharmacology, Faculty of Science, Department of Pharmaceutical Sciences Utrecht, Utrecht University, Utrecht, The Netherlands

[7] Present address: Leiden Academic Centre for Drug Research, Leiden University, Einsteinweg 55, 2333 CC Leiden, The Netherlands

Keywords Lenvatinib · Mass balance · Metabolite identification · Pharmacokinetics · Metabolism · Clinical pharmacology

Abbreviations

2-ME	2-mercaptoethanol
ACN	Acetonitrile
HPLC	High performance liquid chromatography
HR-MS	High-resolution mass spectrometry
LC-MS	Liquid chromatography mass spectrometry
LLOQ	Lower limit of quantitation
LOD	Limit of detection
LSC	Liquid scintillation counting
MeOH	Methanol
TRA	Total radioactivity

Introduction

Lenvatinib is an oral multiple receptor tyrosine kinase inhibitor that inhibits VEGFR1-3, FGFR1-4, PDGFRβ, RET and KIT [1, 2]. The kinase activities of these receptors usually recruit endothelial cells to form new blood vessels, which is important for the development, progression and metastasis of different tumor types. Inhibition of VEGF receptors inhibits tumor progression [3–5]. Currently, lenvatinib is investigated in various Phase II and Phase III clinical trials as monotherapy or as part of a combination therapy for several types of solid tumors, including hepatocellular carcinoma, melanoma, renal carcinoma, non-small cell lung carcinoma, glioblastoma multiforme, ovarian and endometrial carcinoma [6–13]. In February 2015, the FDA approved lenvatinib as a treatment for patients with locally recurrent or metastatic, progressive, radioiodine-refractory differentiated thyroid cancer. In March 2015, the MHLW approved lenvatinib as a treatment for patients of unresectable thyroid cancer. In May 2015, the EMA also approved lenvatinib as a treatment of progressive, locally advanced, or metastatic differentiated thyroid carcinoma in adults whose disease has progressed despite standard treatment with radioactive iodine. The Phase III study of lenvatinib in this type of patients demonstrated significant prolongation of progression free survival (18.3 months versus 3.6 months, hazard ratio 0.21; 99 % confidence interval 0.14–0.31) when lenvatinib was compared to placebo [13, 14]. Lenvatinib is under review for market authorization worldwide.

Preclinical investigation of the metabolism of lenvatinib revealed a variety of biotransformation pathways and the involvement of several enzymes. In one of the metabolic pathways observed in male cynomolgus monkeys is conjugation with glutathione (GSH) under elimination of the chlorophenoxy group, followed by further hydrolysis, rearrangement from S-conjugate to N-conjugate and dimerization [15]. Another pathway, found in rats, dogs, monkeys and humans, involves cytochrome P450 enzymes and results in mono-oxidized metabolites of lenvatinib, such as the N-oxide (M3) and the demethylated metabolite (M2). Also, aldehyde oxidase was demonstrated to play a role in lenvatinib metabolism, but the two resulting oxidative metabolites (M3' and M2') were only found in monkey and human liver fractions and not in rats and dogs (Inoue et al., 2014). These preclinical results suggest a unique metabolic pathway for lenvatinib in humans.

In a previously conducted human mass balance study with ^{14}C-lenvatinib (Fig. 1), 10 days after the initial dose, the geometric mean (CV) recovery of the administered (single oral 24 mg: 100 μCi) dose was 88.6 % (10.4 %). The majority of 63.6 % (11.2 %) was recovered in feces and 24.7 % (17.8 %) in urine [16]. Unchanged lenvatinib in urine and feces accounted for 2.52 % (67.7 %) of the administered dose, indicating a major role for metabolism in the elimination of lenvatinib [16]. Therefore, the objective of present study was to further elucidate the metabolic pathways of lenvatinib in humans and to compare this to the metabolic pathways in rat and monkey. To this end, selected samples collected during the human mass balance study and during lenvatinib metabolism studies in rat and monkey were analyzed using high-performance liquid chromatography (HPLC), followed by off-line radioactivity detection and characterization with a linear ion trap mass spectrometer. The existing knowledge of lenvatinib metabolism was then used in combination with high-resolution mass spectrometry (HR-MS) to identify the metabolites, to describe the extensive biotransformation of lenvatinib in humans and relate this to the metabolism of lenvatinib in rats and monkeys.

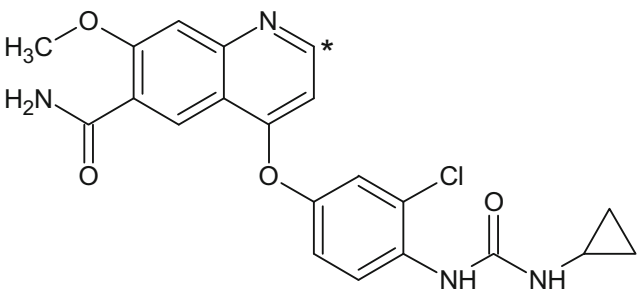

Fig. 1 Chemical structure of ^{14}C-lenvatinib. The asterisk (*) indicates the site labeled with ^{14}C

Materials and methods

Reference standards

Reference standards of Lenvatinib (4-[3-Chloro-4-*N*'-cyclopropylureido)phenoxy]-7-methoxyquinoline-6-carboxamide) methanesulfonate salt, and the lenvatinib metabolites M1 (decyclopropylated lenvatinib), M2 (demethylated lenvatinib), M3 (N-oxidated lenvatinib), M5 (O-dearylated lenvatinib), M3' (2-quinolone form of lenvatinib) and M2' (2-quinolone form of demethylated lenvatinib) were provided by Eisai Co. Ltd. (Tokyo, Japan). Additionally, Eisai Co. Ltd. provided reference standards of the chlorophenol moiety of lenvatinib and its sulphate and glucuronic acid conjugate (referred to as MET29.1, MET24.1 and MET20.1, respectively).

Chemicals

Water (Lichrosolv, used for liquid chromatography), acetic acid (100 %), hydrogen peroxide, dimethylsulfoxide (DMSO, Seccosol), potassium dihydrogen phosphate (KH_2PO_4) p.a., sodium hydroxide (NaOH) 50 %, p.a. and trichloroacetic acid (TCA), p.a. were obtained from Merck (Darmstadt, Germany). Water (used for sample preparation) was obtained from B Braun (Melsungen, Germany). Methanol (Supra-Gradient grade) was purchased from Biosolve Ltd (Amterdam, The Netherlands), 2-propanol from Fluka (Buchs, Switzerland) and ammonium acetate, LC-MS grade from Fluka (Zwijndrecht, The Netherlands). The β-glucuronidase from E.Coli, X-A (7780000 u/g) was supplied by Sigma-Aldrich (St Louis, MO, USA) and both Solvable® and Ultima Gold liquid scintillation cocktail by PerkinElmer (Waltham, MA, USA).

Ethics

The protocol for the human study was approved by the institutional ethics committee, and all human patients provided written informed consent before participating in this study. The human study was conducted in compliance with the principles set forth in the Declaration of Helsinki, International Conference on Harmonization Guideline E6 for Good Clinical Practice and Food and Drug Administration Good Clinical Practice regulations.

All animal studies were approved by the institutional animal care and use committee.

Sample collection

The human samples used in this study were collected during a single-center, open-label, mass balance study of ^{14}C-lenvatinib (Fig. 1), performed in patients with solid tumors or lymphomas at the Antoni van Leeuwenhoek Hospital/The Netherlands Cancer Institute [16]. As described previously [16], six patients with solid tumors or lymphomas received a 24 mg (100 μCi) oral dose of ^{14}C-lenvatinib dissolved in 12 mL of 3 mM hydrochloric acid.

Predose and postdose blood samples were collected in sodium heparin tubes and stored as plasma after centrifugation (4 °C, 15 min, 2000 g). For the present metabolite profiling study only the following samples were analyzed: predose and 1, 2, 4, 8, 12, 24, 48 and 72 h after administration.

Urine was collected once before administration, over 6 h periods during the first 24 h after ^{14}C-lenvatinib administration and over 24 h periods thereafter. In the present study, the predose sample and pooled urine samples over 0–24, 24–48, 48–72 and 72–168 h were analyzed for each patient, to investigate the metabolism of ^{14}C-lenvatinib in humans over time. To compare the human metabolites with those in rat and monkey, one inter-patient pool of the predose samples and one inter-patient pool of the 0–6 h samples was used.

Feces was collected before dosing and as voided until radioactivity was <1 % of the administered dose. In the present study, the predose sample and pooled feces samples over 0–24, 24–48, 48–72 and 72–168 h were analyzed for each patient. The human fecal sample with the highest concentration of radioactivity was used to compare the human metabolites with metabolites found in rat and monkey. All samples were stored at −70 °C pending metabolite profiling analysis.

The cynomolgus monkey samples used in this study were collected during a metabolite profiling study of ^{14}C-lenvatinib in rats and monkey by Eisai Co., Ltd, Ibaraki, Japan [15]. The monkey received repeated oral administrations (once a day for 2 days) of ^{14}C-lenvatinib at a dose of 30 mg (12.685 MBq)/kg. Urine and feces were collected separately, as voided in a receiver on an ice bath and in the dark, during specified time periods. In the present study, only the urine and fecal samples collected predose and 0–24 h postdose were investigated.

The rat samples used in this study were collected during the same metabolite profiling study of ^{14}C-lenvatinib in rats and monkey. The male Sprague Dawley rats received a single oral administration of ^{14}C-lenvatinib at a dose of 30 mg (12.685 MBq)/kg. Urine and feces were collected separately, as voided in a receiver on an ice bath and in the dark, during specified time periods. Biliary samples were collected from bile duct cannulated male Sprague–Dawley rats, which received the same dose of ^{14}C-lenvatinib. Bile was collected in a light protected receiver on an ice bath during specified time periods. In the present study, only one urine and fecal sample collected predose and 0–24 h postdose and one bile sample collected predose and 0–8 h postdose were investigated.

Both monkey and rat samples were stored at −80 °C and transported to the Netherlands Cancer Institute pending metabolite profiling analysis.

Analysis of radioactivity

The radioactivity of the samples and collected HPLC-fractions was measured with a liquid scintillation counter (LSC) Model TRI-CARB 2800 TR (Perkin Elmer Life and Analytical Sciences, Inc., Waltham, MA), equipped with a quenching correction system. After sample preparation (if necessary, as described in the next section), the samples were mixed with scintillation cocktail and counted for 20 min.

Preparation of biological samples for metabolite profiling

The preparation of all matrices is further described in a flow chart in Fig. 2.

Plasma

Human plasma samples of 300 µL were extracted twice by adding 150 µL of water and 900 µL of methanol, vortex mixing (10 s), shaking (10 min) and centrifuging (4 °C, 10 min, 23,100 g). The residue (pellet 1) was kept for recovery measurements. The combined supernatants were dried under nitrogen at 40 °C and reconstituted by addition of 40 µL of methanol and 160 µL of 0.1 M phosphate buffer (pH 7.4) with 30 s vortex mixing after each addition. This mixture was centrifuged again (4 °C, 10 min, 23,100 g) and the residue (pellet 2) was kept for recovery measurements. A 20 µL volume of the supernatant was used for recovery analysis using LSC and the remainder was transferred to an autosampler vial and stored at −70 °C until analysis with LC-LSC-MS.

Additional extractions were performed on pellet 1. First by addition of 900 µL of 15 % trichloroacetic acid (TCA), followed by vortex mixing, shaking and centrifuging as described above, second by addition of 900 µL methanol, followed by vortex mixing, shaking, incubating at 60 °C for 10 min, vortex mixing and centrifuging. Both the TCA supernatant and the methanol supernatant were analyzed for total radioactivity using LSC, as were the final remainder of pellet 1 after solubilization using Solvable® and pellet 2 after dissolving in 200 µL methanol.

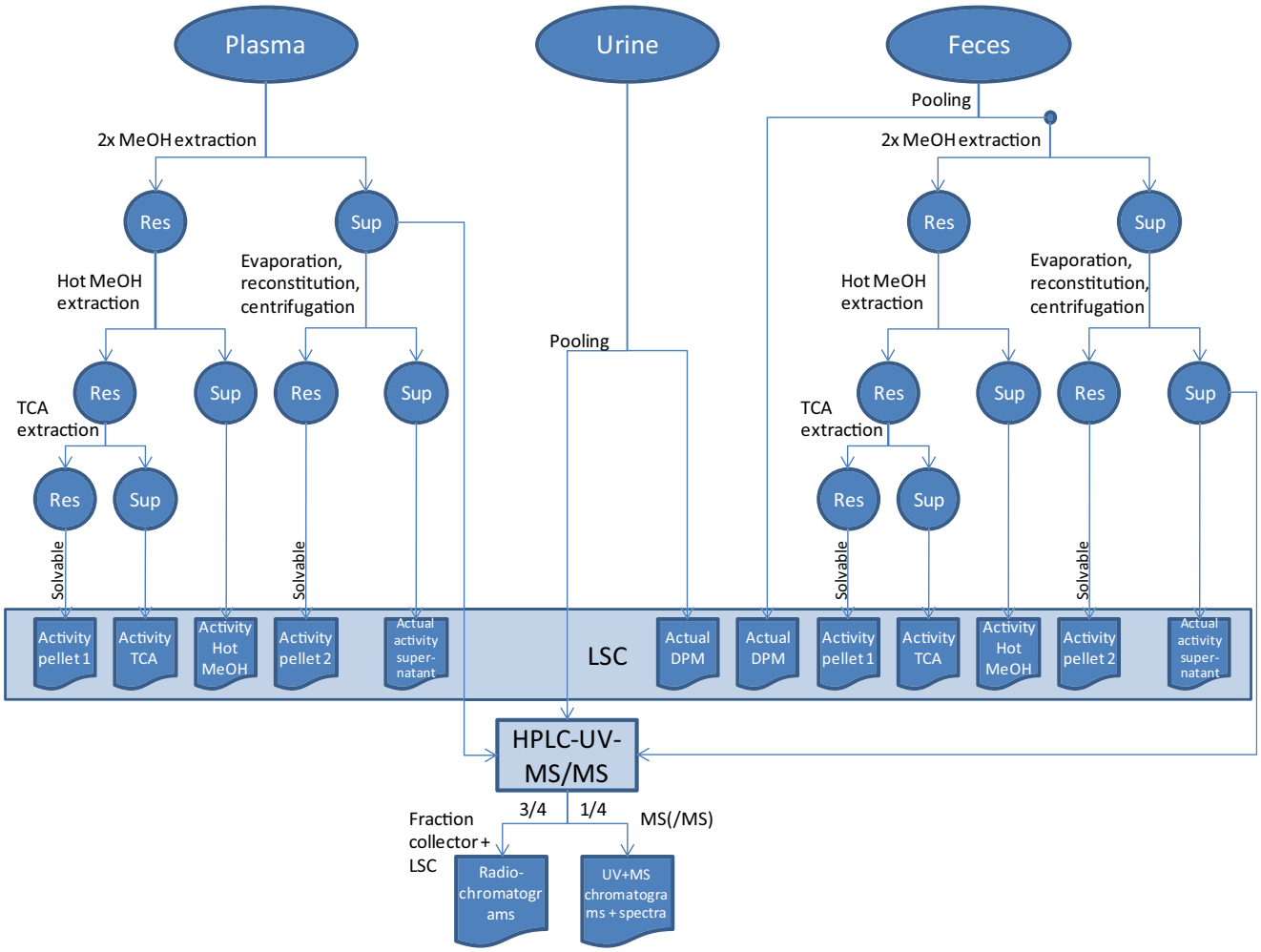

Fig. 2 Sample preparation flow chart of plasma, urine and feces samples

Treatment with 2-mercaptoethanol

Unextracted radioactivity after sample pretreatment in plasma samples were extracted by treatment with 2-mercaptoethanol (2-ME), to reduce potential sulfur bridges between proteins and lenvatinib-related compounds. After sample preparation, this included extraction with methanol and treatment of the remaining pellet with trichloroacetic acid (TCA) and hot methanol, the remaining pellet was incubated with 2-ME. For the extraction of plasma samples an aliquot of 300 μL plasma was used. After the TCA and methanol extractions, 20 % 2-ME in water (2:8, v/v) was added to the remaining pellet and incubated for 2 h at 60 °C. The sample was cooled, mixed and centrifuged (RT, 3000 rpm, 10 min). The supernatant was evaporated under nitrogen at 40 °C. The pellet was washed with methanol after which the methanol was added to the supernatant and evaporated. The dried supernatant was reconstituted with methanol and 0.1 M phosphate buffer pH 7.4 (1:5, v/v) to obtain an HPLC sample. The recovery of the radioactivity from the 2-ME extraction was calculated by comparing the radioactivity concentration in feces and in the HPLC sample (supernatant). The remaining pellet after 2-ME extraction was decolorized and solubilized and the total radioactivity of the pellet was determined.

Urine

The human urine samples of individual patients were directly injected onto the HPLC system. The urine samples pooled across patients were 30-fold concentrated by lyophilization in a freeze dryer (2040, Snijders, Tilburg, The Netherlands) and reconstitution with water, after which the samples were centrifuged (RT, 23,100× *g*, 5 min) to obtain supernatant as an HPLC sample. An aliquot of the HPLC sample was subjected to the radioactivity measurement by LSC. The sample preparation recovery was calculated by comparing the radioactivity concentration in the pooled urine sample before lyophilization and in the final HPLC sample.

Urine samples from rats and the monkey were vortex mixed and diluted without additional preparation. The recovery was not determined for these samples.

Treatment with β- glucuronidase

To identify glucuronide-conjugated metabolites, one 200 μL aliquot of the lyophilized and concentrated pooled human urine sample of 0–6 h postdose was mixed with 200 μL phosphate buffer (pH6.8) and served as a control sample and another 200 μL aliquot was mixed with 35 μL of 1 mg/mL β-glucuronidase and 165 μL of phosphate buffer (pH6.8). Both aliquots were incubated for 24 h at 37 °C, after which they were diluted with 5 volumes of methanol, vortex mixed and stored at −70 °C until analysis.

Feces

Human, monkey and rat fecal homogenate aliquots of 200 μL were extracted twice using 0.1 M phosphate buffer (pH 7.4) and methanol in volume ratios of 1:1:4, followed by vortex mixing, shaking (10 min) and centrifuging (10 min, 4 °C, 20, 000 g). The residue (pellet 1) was kept and the combined supernatants were evaporated to dryness under nitrogen at 30 °C and reconstituted in 150 μL of methanol:water 1:1 v/v, followed by vortex mixing for 30 s, sonicating for 5 min and vortex mixing for 30s. A 20 μL aliquot was mixed with scintillation cocktail and analyzed for total radioactivity. The remainder was centrifuged (5 min, 4 °C, 20,000 g), the residue (pellet 2) was kept and a 20 μL aliquot of the final extract (the supernatant) was analyzed for total radioactivity. Conform safety regulations, the final extract (and the final extract of the corresponding predose sample) was, if necessary, diluted with methanol:water 1:1 v/v to a final radioactive concentration below 10^4 Bq/mL and used for LC-LSC-MS analysis.

Each pellet 1 and an aliquot of each non-treated fecal homogenate was analyzed for total radioactivity after decolorization and solubilization using isopropanol, hydrogen peroxide and Solvable® as described [16]. Each pellet 2 was analyzed for total radioactivity using LSC after dissolving in 1 mL of methanol.

Treatment with 2-mercaptoethanol

Unextracted radioactivity after sample pretreatment in feces samples were also extracted by treatment with 2-mercaptoethanol (2-ME). For the extraction in feces samples an aliquot of 1 mL feces homogenate was used. The remaining procedure was similar as described previously.

Bile

The bile collected from rats was diluted with methanol:water 1:1 v/v to a final radioactive concentration below 10^4 Bq/mL and used for LC-LSC-MS analysis.

Radiochromatographic detection of metabolites of lenvatinib

Initially the human samples and animal samples were analyzed on two different locations and therefore two chromatographic methods were developed and applied during this study. The methods had a total run time of 60 min (this method will be referred to as method 1) and 73 min (This method will be referred to as method 2). The samples that were used for the inter-species comparison (i.e. urine, feces and bile) were analyzed using both methods. The human plasma samples were analyzed on method 1 only.

The LC-LSC-MS setup was the same for both methods: an Accela pump and autosampler (4 °C) (Thermo Electron, Waltham, MA, USA) with a sample loop allowing 50 uL injections onto the HPLC column which was preceded by an 0.2 μm inlet filter (Upchurch Scientific, Oak Harbor, WA, USA) and warmed to 30 °C. The 1 mL/min flow was split post-column using an Accurate splitter (LC packings, Sunnyvale, CA, USA), directing ¼ of the flow to the mass spectrometer and ¾ of the flow to a fraction collector (LKB-FRAC-100, Amersham Biosciences AB, Uppsala, Sweden), collecting 1 or 5 min fractions in liquid scintillation vials. After addition of scintillation cocktail (4 mL to the 1 min fractions and 10 mL to the 5 min fractions), the total radioactivity of each fraction was determined on the Tri-carb 2800TR liquid scintillation counter, using a counting time of 20 min. The resulting values were used to construct the radiochromatograms.

Method 1 used a Synergy Hydro RP 80A column (150 × 4.6 mm ID with 4 μm particles, Phenomenex, Torrance, CA, USA), with 10 mM ammonium acetate as mobile phase A and methanol as mobile phase B. The gradient started at 5 % B for 5 min, increased to 80 % B over 45 min and increased further to 90 % B over 2 min, where it stayed until 54.9 min, in order to return to the starting conditions within 0.1 min, until the end of the run.

Method 2 applied an Atlantis T3 column (150 × 4.6 mm ID with 5 μm particles, Waters Corp., Milford, MA, USA). In this method, mobile phase A consisted of 100 mM ammoniumacetate / water / formic acid 100/900/0.5 v/v/v and mobile phase B of 100 mM ammoniumacetate / acetonitrile / formic acid 100/900/0.5 v/v/v. The gradient started at 0 % B and increased to 15 % B over 15 min, then to 30 % B over 35 min, and to 100 % B over 1 min, where it stayed until 65 min, in order to return to the starting conditions within 0.5 min, until the end of the run.

Mass spectrometry for metabolite identification

An LTQ XL (Thermo Electron, Waltham, MA) ion trap mass spectrometer was used for the LC-LSC-MS analyses, applying positive ionization and using a scan range of 100 to 1100 amu. The sheath, auxiliary and sweep gas flows were 30, 15 and 5 arbitrary units. The spray voltage was 5.4 kV, the normalized collision energy was 45 V and Data Dependent Acquisition was performed to collect MS^2 and MS^3 data using a predefined parent list (based on preliminary data) with a threshold of 750 cps and 100 cps, respectively.

In addition the samples were analyzed using LC-MS/MS with mass spectrometric detection by an LTQ Orbitrap XL (Thermo Electron, Waltham, MA) to collect high resolution MS (HR-MS) and MS^2 data. All settings were similar to the settings of the LTQ XL except for the normalized collision energy which was 40 eV. Non-radiolabeled metabolites of lenvatinib were also analyzed using negative ionization. All other settings were kept the same.

Calculations

The limit of detection (LOD) of the total radioactivity measurements was calculated with formula (1) [17]:

$$LOD = \frac{2.71}{TE} + 4.65\sqrt{\frac{B}{TE}} \quad (1)$$

With a counting time (T) of 20 min, an observed background (B) of 11.0 DPM (disintegrations per minute) and a counting efficiency (E) of 93 % the LOD is 3.7 DPM, which was rounded to 4 DPM.

At the lower limit of quantification (LLOQ) a maximum precision error of 20 % was considered acceptable, allowing to use formula (2) to calculate the LLOQ after background correction [18]:

$$LLOQ = \frac{50}{TE}\left(1 + \sqrt{1 + \frac{2TEB}{25}}\right) \quad (2)$$

Using the same values for T, E and B as before, the calculated LLOQ was 14 DPM.

The area under the concentration time curve from 0 to 24 h after drug administration ($AUC_{0\text{-}24h}$) was calculated with the trapezoidal rule (3), using time since administration and concentration at data point i (t_i and C_i, respectively) and n as the total number of data points:

$$AUC_{(0-24h)} = \sum_{i=0}^{n-1} \frac{t_{i+1} - t_i}{2} \times (C_i + C_{i+1}) \quad (3)$$

Results

The results describe the identification of metabolites found in humans and the quantification of these metabolites in human plasma, urine and feces. In addition the metabolic pathway in humans is compared to the metabolic pathway in rat and humans.

Lenvatinib metabolism in human

Metabolites in plasma

The sample preparation recovery of total radioactivity in human plasma is summarized in Fig. 3a, which shows that the recovery decreased with increasing collection time. The samples collected up to 24 h had a mean recovery in the final supernatants of 74 %. The losses are mainly recovered upon

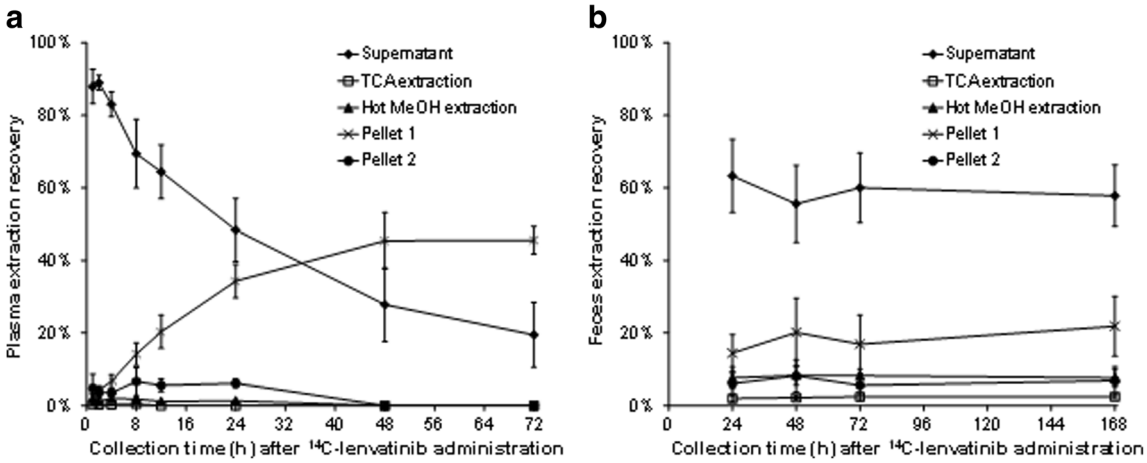

Fig. 3 Mean (± standard deviation) of sample preparation recoveries of human plasma samples (**a**) and human feces samples (**b**) collected from patients following a single oral dose of 24 mg (100 μCi) ^{14}C-lenvatinib ($n = 6$)

solubilization of pellet 1, the pellet remaining after extractions with TCA and hot methanol, which recovered only negligible amounts of radioactivity. Up to 24 h, a mean of 5 % of the total radioactivity was recovered in pellet 2, which was left after reconstitution of the dried sample. Of the radioactivity that was injected on the HPLC column, a mean of 80 % was detected in the collected fractions. The recovery of radioactivity from pellet 1 after 2-ME treatment was below the LOD and therefore no further metabolite identification was possible.

Plasma radiochromatograms were only constructed for plasma samples collected up to 24 h, because the radioactivity in the final supernatants of samples collected later was (with 5–43 DPM in total) considered insufficient. Figure 4a and b show representative plasma radiochromatograms. A similar profile is observed in all analyzed samples of all 6 patients: lenvatinib was the main peak in each chromatogram, accounting for a mean of 97 % of the radioactivity in the chromatograms. Small amounts of radioactivity (mean of 2.5 %) eluted in fraction 31 and were identified as MET27 (glucuronic acid conjugate of M2), as described under *metabolite identification*. On average 0.53 % of the radioactivity in plasma chromatograms was not accounted for.

The mean $AUC_{0\text{-}24h}$ of MET27 was 3.2 % of the lenvatinib $AUC_{0\text{-}24h}$ and 1.8 % of the total ^{14}C $AUC_{0\text{-}24h}$. The $AUC_{0\text{-}24h}$ of MET27 did not exceed 4.9 % of the lenvatinib $AUC_{0\text{-}24h}$ and 2.8 % of the total ^{14}C $AUC_{0\text{-}24h}$ for any patient.

Metabolites in urine

The time-pooled urine samples of six patients were analyzed using LC-LSC-MS method 1. The mean HPLC column recovery of the total radioactivity was 95 %.

A mean of 23 % of the total radioactivity that was administered to the patients was recovered in the urine sample pools up to 168 h. Figure 4c and d show a representative radiochromatogram of a 0–24 h sample and a 72–168 h sample, respectively. At least 10 peaks other than lenvatinib were observed. These were named MET4 (accounting for 6.8 % of the administered radioactive dose), A (accounting for 0.78 %), B (0.99 %), D (3.7 %), E (0.68 %), MET24 (0.98 %), MET31 (0.44 %), MET27 (1.8 %), M3' (0.49 %) and M2 (accounting for 0.13 % of the administered radioactive dose). Unchanged lenvatinib comprised 0.38 % of the administered dose and the remaining 6.1 % of the dose was recovered in the urine radiochromatograms but not assigned to a metabolite.

The most abundant metabolite MET4 was tentatively identified as a cysteine-adduct of the quinolone moiety of lenvatinib. Other tentatively identified metabolites included lenvatinib products of demethylation (M2) or oxidation (M3') and their glucuronic acid conjugates (MET27 and MET31, resp.). No parent mass was found for the peaks assigned with letters, and consequently these were not identified.

Metabolites in feces

The time-pooled feces samples of six patients were prepared and analyzed using LC-LSC-MS method 1. The sample preparation recovery of total radioactivity in feces samples is summarized in Fig. 3b. Contrary to the extraction recovery of plasma samples, the extraction recovery of feces remained constant over collection time. The mean extraction recovery over all patients was 59 % and a large inter-patient variability was observed (range of 47–70 %). Subsequent extraction of pellet 1 with TCA and hot methanol recovered an additional mean of 2.2 and 7.9 %, respectively, of the total radioactivity in the initial sample. A mean of 18 % of the initial total radioactivity was found in pellet 1 after solubilization and 6.7 % in

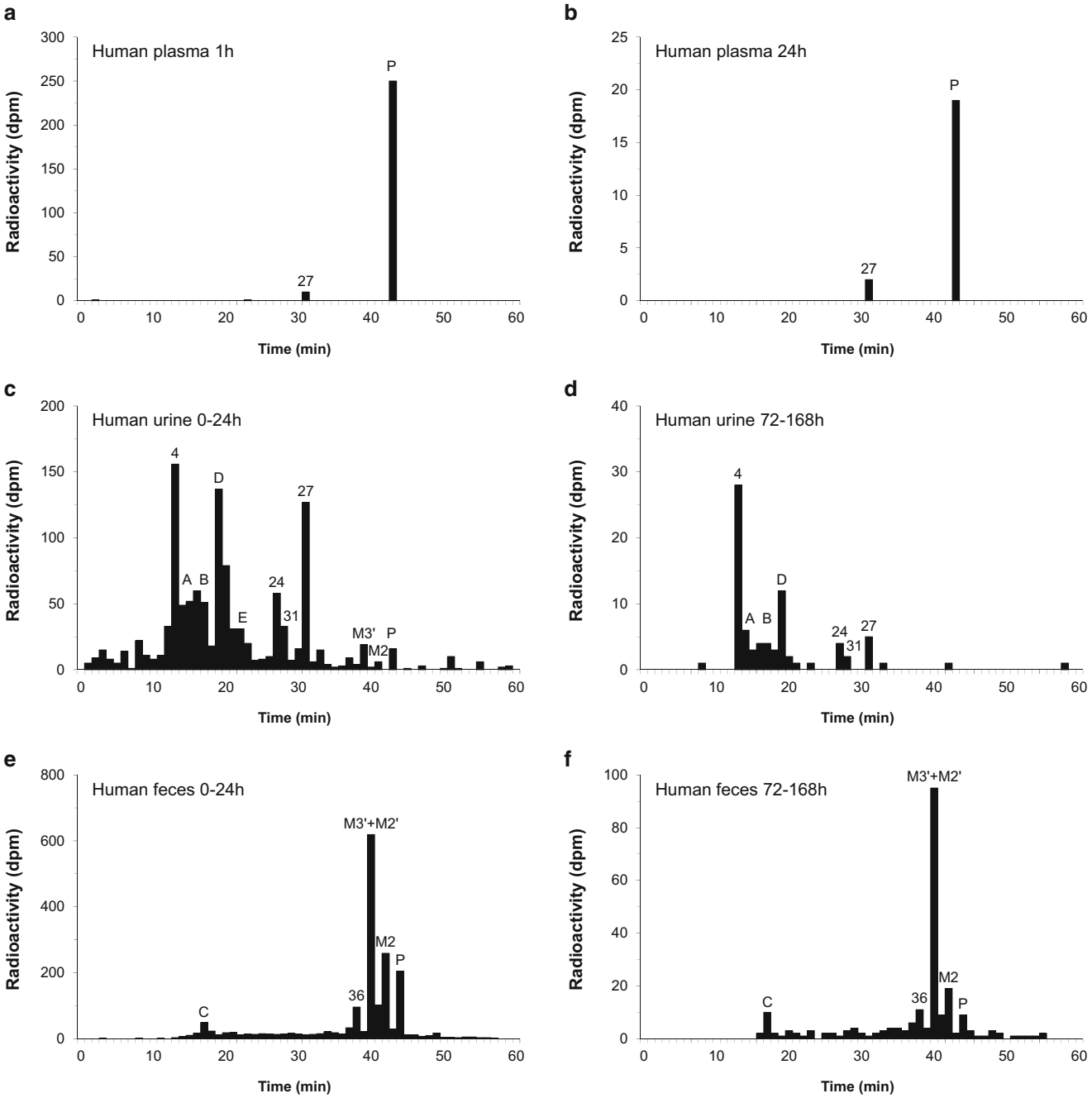

Fig. 4 Representative radiochromatograms of human plasma collected 1 h (**a**) and 12 h (**b**), human urine collected over 0–24 h (**c**) and 72–168 h (**d**) and human feces collected over 0–24 h (**e**) and 72–168 h (**f**) after administration of a single oral dose of ^{14}C-lenvatinib. The numbers in the radiochromatograms correspond with the MET-numbers in the text; the prefix MET was omitted due to space restrictions

pellet 2. The mean HPLC column recovery of the total radioactivity was 101 %. After 2-ME treatment the majority of the non-extracted radioactivity in pellet 1 was found in the 2-ME extract (mean of 11 %).

A mean of 65 % of the radioactivity administered to the patients was excreted in the feces pools up to 168 h. To calculate the percentage of the administered radioactive dose recovered as a metabolite in feces, the radiochromatographic peaks were corrected for the sample extraction recovery which will be discussed later. Figure 4e and f show a representative radiochromatogram of a 0–24 and a 72–168 h feces pool. At least 4 peaks other than lenvatinib were observed. These were assigned as C, MET36, M3', M2' and M2 and these comprised 3.4, 2.8, 16, 11 and 4.3 % of the administered dose,

respectively. M3' and M2' eluted in the same fraction, therefore only their combined contribution of the administered dose could be determined from the radiochromatograms. The individual contributions were based on their LC-MS signal intensity, assuming comparable ionization efficiencies for both compounds. Unchanged lenvatinib accounted for 2.5 % of the administered dose and the remaining 25 % of the dose was recovered in the feces radiochromatograms but not assigned to a metabolite. While no molecular weight, and therefore no identity was found for metabolite C, the other metabolites were tentatively identified as products of oxidation (MET36, M3'), demethylation (M2), or both (M2'). In the 2-ME extract a trace of two proposed compounds were found; demethylated 2-hydroxyethanethiolate conjugate of the quinoline moiety of lenvatinib (MET43) and its demethylation product (MET42).

Comparison of lenvatinib metabolites in rat, monkey and human

In order to get a more complete picture of lenvatinib metabolism and to compare the presence of lenvatinib metabolites in different species, selected samples of a ^{14}C-lenvatinib mass balance study in rat, monkey and human were analyzed using LC-LSC-MS method 1 and 2 and matching predose samples were analyzed using LC-MS. The sample preparation recovery in the postdose fecal extracts were 80, 78 and 54 % for rat, monkey and human, respectively.

Figure 5 shows the radiochromatograms of each matrix analyzed with method 2. Many metabolites that were found in the earlier described human metabolism study were also detected in the animal samples. The drug-related products assigned A, B, C, D and E were detected in human study samples, but as no molecular ion was found for these compounds, their presence nor absence could be confirmed in the animal samples.

The most abundant radiolabeled metabolite in rat urine was an N-acetylcysteine adduct of the quinolone moiety (MET18). In rat feces, unchanged lenvatinib comprised the majority of the lenvatinib related radioactivity. The major metabolites in rat bile were a glutathione adduct of the quinolone moiety of lenvatinib (MET15), the N-linked and S-linked isomers of cysteinylglycine adducts of the quinoline moiety of lenvatinib (MET19A and MET19B), the glucuronic acid conjugate of M2 (MET27), the N-oxide of lenvatinib (M3) and unchanged lenvatinib.

In monkey urine, the most abundant radiolabeled metabolite was a dimer of cysteine adducts to the quinoline moiety (MET16) and was identified previously by Inoue et al. using LC-MS^n and NMR (Inoue et al., 2012). As a dimer may contain 2 radiolabels, the presence of this metabolite may be slightly overestimated. In monkey feces, unchanged lenvatinib comprised the majority of the lenvatinib-related radioactivity.

The most abundant radiolabeled metabolites in human urine were a cystine adduct to the quinoline moiety of lenvatinib (MET4), a glucuronic acid conjugate of M2 (MET27) and the unidentified metabolite D. In human feces, only a limited amount of unchanged lenvatinib was detected. The major radioactive components in feces were the demethylated derivative of lenvatinib (M2), the quinolinone form of lenvatinib (M3') and a combination of those (M2'), together with the unidentified metabolite MET41.

Apart from the radiolabeled metabolites, also non-radiolabeled metabolites were detected in the samples by comparison of the predose and postdose LC-MS chromatograms. The non-radiolabeled glucuronic acid conjugate of the chlorophenol moiety of lenvatinib (MET20.1) produced high intensity peaks in the extracted ion chromatograms of rat, monkey and human urine, suggesting that this is also a major metabolite of lenvatinib.

Identification of metabolites

LC-MS^n was the primary tool to generate the profiles of the metabolites and to elucidate the structures of the metabolites. The structures were proposed based on the (if available high-resolution) mass of molecular ions, fragmentation patterns and on comparison of the HPLC retention times and fragmentation patterns with those of the available reference standards. High-resolution spectra and proposed fragmentation of the most abundant metabolites (MET4, MET27, M2, M3' and M2') are included in Supplementary Figure 1. Table 1 shows an overview of the structural information obtained by LC-MS^n for the lenvatinib metabolites that were elucidated in biological samples of human, monkey and rat. The metabolite numbers are assigned according to the retention time of the metabolite except for metabolites MET42 and MET43 and lenvatinib metabolites reported and assigned in earlier publications (M1, M2, M3, M5, M2' and M3'), which were named by their original assignment [16, 19, 20]. Proposed metabolic schemes are illustrated in Figs. 6 and 7. The rationale for structural characterization is described below. Here the identification of the most abundant metabolites in human are described. The identification of the other metabolites are described in Supplementary Data 1.

Lenvatinib

The identity of lenvatinib was confirmed with the reference standard of lenvatinib. The protonated molecular ion at *m/z* 427.1161 gave product ions at *m/z* 410.0896, 370.0582, 344.0790 and 327.0527 corresponding to the loss of an amine, loss of a cyclopropylamine, loss of a cyclopropylformamide and loss of an amine and cyclopropylformamide, respectively.

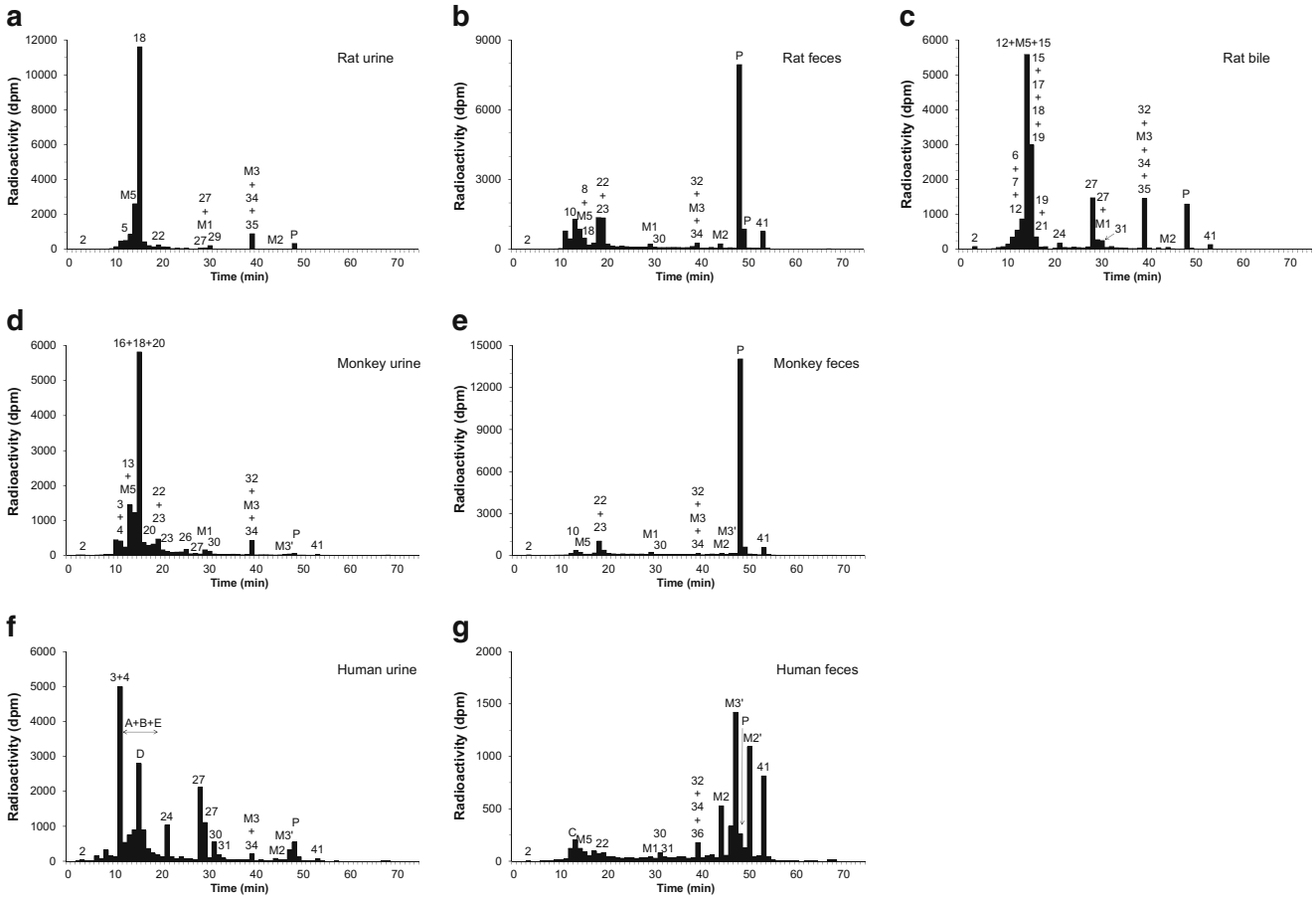

Fig. 5 Radiochromatograms of rat urine (**a**), feces (**b**) and bile (**c**), of monkey urine (**d**) and feces (**e**) and human urine (**f**) and feces (**g**) collected after administration of a single oral dose of ^{14}C-lenvatinib. The urine profiles were obtained from urine collected in the 0 to 24 h (rat and monkey) or 0 to 6 h (*human*) interval after dose administration, the feces profiles from feces collected in the 0 to 24 h interval (*rat*) and 24 to 48 h interval (*monkey and human*) and the bile profile from bile collected in the 0 to 6 h interval after dose administration. The numbers in the radiochromatograms correspond with the MET-numbers in the text; the prefix MET was omitted due to space restrictions

Metabolite MET4

MET4 had a protonated molecular ion at *m/z* 441.0890. The MS-spectra and proposed fragmentation are included in Supplementary Figure 1. The major product ions were detected at *m/z* 424.0621 (loss of NH_3), *m/z* 396.0677 (loss of HCO_2), *m/z* 354.0570 (loss of alanine moiety), *m/z* 320.0694 (loss of cysteine moiety), *m/z* 288.0975 (loss of thiocysteine moiety) and *m/z* 244.1072 (loss of both thiocysteine moiety and CO_2). The proposed identity is a cystine adduct of the quinoline moiety of lenvatinib.

Metabolite MET27

MET27 had a protonated molecular ion at *m/z* 589.1325. The MS-spectra and proposed fragmentation are included in Supplementary Figure 1. The major product ions were detected at *m/z* 413.1002 (loss of pyroglucuronic acid) and *m/z* 330.0630 (loss of pyroglucuronic acid and cyclopropylformamide). The MS^3 spectrum of the product ion at *m/z* 413 (loss of pyroglucuronic acid) showed fragments of *m/z* 396 (additional loss of NH_3), *m/z* 356 (additional loss of cyclopropylamine), *m/z* 330 (additional loss of cyclopropylformamide) and *m/z* 313 (additional loss of cyclopropylformamide and NH_3). This MS^3 spectrum was identical to the MS^2 spectrum of M2 (*O*-desmethyl lenvatinib). The proposed identity of this metabolite is a glucuronic acid conjugate of M2, which was confirmed by incubation with β-glucuronidase.

Metabolite MET36

MET36 had a protonated molecular ion at *m/z* 459.1064 with a fragment *m/z* 441.0953 (loss of water) also present in the MS^1 spectrum. The MS^2 spectrum of *m/z* 459 showed one product ion at *m/z* 441 (loss of water). The MS^2 spectrum of *m/z* 441 was identical to the MS^3 spectrum of the product ion at *m/z* 441, formed from *m/z* 459. They showed one product ion at *m/z* 424.0686 (loss of NH_3). The MS^3 spectrum of *m/z* 424 formed from the product ion of *m/z* 441 (hypothetically

Table 1 Overview of structural information obtained by LC-MS^n for lenvatinib metabolites detected in biological samples of rat, monkey and human

Name	Description proposed identity	Formula	Calculated *m/z*	Observed *m/z*	Mass error (ppm)	Major fragment	Species	Structure characterization	Ref.*
P	Lenvatinib	$C_{21}H_{20}ClN_4O_4^+$	427.1168	427.1161	−1.6	410, 370, 344, 327	Human, monkey, rat	Confirmed by authentic standard	[15, 16, 19]
MET1	Unknown	Unknown	Unknown	Unknown	NA		–		
MET2	Unknown	Unknown	Unknown	Unknown	NA		–		
MET3	Cystinylglycine adduct of the quinoline moiety of lenvatinib	$C_{19}H_{24}N_5O_7S_2^+$	498.1112	498.1114	0.4	481, 453, 411, 377, 345, 320	Human, monkey	Proposed	
MET4	Cystine adduct of the quinoline moiety of lenvatinib	$C_{17}H_{21}N_4O_6S_2^+$	441.0897	441.0890	−1.6	354, 320, 288	Human, monkey	Proposed	
MET5	Unknown	Unknown	Unknown	269.1491	NA	277, 164	Rat		
MET6	Glutathione disulfanyl cysteinylglycine adduct of the quinoline moiety of lenvatinib	$C_{26}H_{34}N_7O_{11}S_2^+$	684.1752	684	NA	555, 411, 377	Rat	Proposed	
MET7	γ-Glutamyl-cysteine adduct of the quinoline moiety of lenvatinib	$C_{19}H_{23}N_4O_7S^+$	451.1282	451	NA	322, 305, 235	Rat	Proposed	
MET8	Sulfonic acid of the quinoline moiety of lenvatinib	$C_{11}H_{11}N_2O_5S^+$	283.0383	283	1.1	266, 202	Rat	Proposed	
MET9	Glutathione disulfanyl cysteine adduct of the quinoline moiety of lenvatinib	$C_{24}H_{31}N_6O_{10}S_2^+$	627.1538	NA	NA	498, 354, 244	Monkey (liver)	Proposed	
A	Unknown	Unknown	Unknown	Unknown	NA	-	-		
B	Unknown	Unknown	Unknown	Unknown	NA	-	-		
C	Unknown	Unknown	Unknown	Unknown	NA	-	-		
MET10	Sulfinic acid of the quinoline moiety of lenvatinib	$C_{11}H_{11}N_2O_4S^+$	267.0434	267.0434	0.0	249, 232, 219	Monkey, rat	Proposed	
MET11	Unknown	Unknown	Unknown	Unknown	NA	-	-		
MET12	*S*-linked cysteine adduct of the quinoline moiety of lenvatinib	$C_{14}H_{16}N_3O_4S^+$	322.0856	322	NA	305, 235	Rat	Proposed	
MET13	Mercaptoacetic acid conjugate of the quinoline moiety of lenvatinib	$C_{13}H_{13}N_2O_4S^+$	293.0591	293.0587	−1.4	276, 249, 232, 216, 204	Monkey	Proposed	[15]
M5	O-deschlorobenzyl lenvatinib	$C_{11}H_{11}N_2O_3^+$	219.0764	219.0761	−1.4	202	Human, monkey, rat	Confirmed by authentic standard	[16]
MET15	Glutathione adduct of the quinoline moiety of lenvatinib	$C_{21}H_{26}N_5O_8S^+$	508.1497	508	NA	291, 433, 379, 235	Rat	Proposed	[15]
MET16		$C_{28}H_{29}N_6O_8S_2^+$	641.1483	641.1484	0.2	354, 288, 244	Monkey	Proposed	[15]

Table 1 (continued)

Name	Description proposed identity	Formula	Calculated *m/z*	Observed *m/z*	Mass error (ppm)	Major fragment	Species	Structure characterization	Ref.*
	Dimer of the cysteine adducts to the quinoline moiety of lenvatinib								
D	Unknown	Unknown	Unknown	224	NA	–	–		
MET17	Dimer of the cysteinylglycine adducts of the quinoline moiety of lenvatinib	$C_{32}H_{35}N_8O_{10}S_2^+$	755.1912	755	NA	738, 411, 379	Rat	Proposed	
MET18	N-acetylcysteine adduct of the quinoline moiety of lenvatinib	$C_{16}H_{18}N_3O_5S^+$	364.0962	364.0960	−0.5	347, 235	Monkey, Rat	Proposed	
MET19	Structural isomers of cysteinylglycine adducts of the quinoline moiety of lenvatinib (*N*-linked or *S*-linked)	$C_{16}H_{19}N_4O_5S^+$	379.1071	379.1068	−0.8	262, 333, 276, 235, 218	Rat	Proposed	
MET20	Heterodimer of the cysteine adduct of the quinoline moiety of lenvatinib and the cysteinylglycine adduct of the quinoline moiety of lenvatinib	$C_{30}H_{32}N_7O_9S_2^+$	698.1697	698	NA	411, 244	Monkey	Proposed	[15]
E	Unknown	Unknown	Unknown	Unknown	NA	–	–		
MET 20.1	Glucuronic acid conjugate of the chlorophenol moiety of lenvatinib	$C_{16}H_{20}ClN_2O_8^+$	403.0903	403.0900	−0.7	277	Human, monkey, rat	Confirmed by authentic standard	
MET 21	*N*-linked cysteine adduct of the quinoline moiety of lenvatinib	$C_{14}H_{16}N_3O_4S^+$	322.0856	322	NA	276, 244, 218, 161	Rat	Proposed	[15]
MET 22	Cysteine adduct to two molecules of the quinoline moiety of lenvatinib, linked with the thiol and amino groups of one molecule of cysteine	$C_{25}H_{24}N_5O_6S^+$	522.1442	522.1436	−1.1	505, 244	Human, monkey rat	Proposed	[15]
MET 23	Cysteinylglycine adduct to two molecules of the quinoline moiety of lenvatinib, linked with the thiol and amino groups of one molecule of cysteinylglycine	$C_{27}H_{27}N_6O_7S^+$	579.1656	579.1656	0.0	562, 534, 516	Monkey, rat	Proposed	
MET24		$C_{22}H_{21}ClN_3O_9^+$	506.0961	506.0962	0.2	330, 313	Human, rat	Proposed	

Table 1 (continued)

Name	Description proposed identity	Formula	Calculated *m/z*	Observed *m/z*	Mass error (ppm)	Major fragment	Species	Structure characterization	Ref.*
	Glucuronic acid conjugate of the aniline derivative of lenvatinib								
MET 24.1	Sulfate conjugate of the chlorophenol moiety of lenvatinib	$C_{10}H_{12}ClN_2O_5S^+$	307.0150	307.0149	−0.3	289, 247, 216	Monkey, rat	Confirmed by authentic standard	
MET25	Unknown	Unknown	Unknown	585.1165	NA	–	–		
MET26	Methyl sulfoxide conjugate of the quinoline moiety of lenvatinib	$C_{12}H_{13}N_2O_3S^+$	265.0641	265.0640	−0.4	247, 130	Monkey	Proposed	
MET27	Glucuronic acid conjugate of M2	$C_{26}H_{26}ClN_4O_{10}^+$	589.1332	589.1325	−1.2	413, 330	Human, monkey, rat	Proposed	
M1	*N*-descyclopropyl lenvatinib	$C_{18}H_{16}ClN_4O_4^+$	387.0855	387.0850	−1.3	370, 344	Human, monkey, rat	Confirmed by authentic standard	[16]
MET29	Quinolinone form of the aniline derivative of lenvatinib	$C_{17}H_{15}ClN_3O_4^+$	360.0746	360.0743	−0.8	343, 237	Rat	Proposed	
MET 29.1	Chlorophenol metabolite of lenvatinib	$C_{10}H_{12}ClN_2O_2^+$	227.0582	227.0579	−1.3	209, 158	Human, monkey, rat	Confirmed by authentic standard	
MET30	Carboxylic acid metabolite resulting from hydrolysis of the amide moiety of lenvatinib	$C_{21}H_{19}ClN_3O_5^+$	428.1008	428.1007	−0.2	410, 371	Human, monkey, rat	Proposed	
MET31	Glucuronic acid conjugate of M3’	$C_{27}H_{28}ClN_4O_{11}^+$	619.1438	619	NA	602, 536, 443, 426, 360	Human	Proposed	
MET32	Aniline derivative of lenvatinib	$C_{17}H_{15}ClN_3O_3^+$	344.0796	344.0792	−1.2	327, 312	Human, monkey, rat	Proposed	
M3	*N*-oxide on the quinoline moiety of lenvatinib	$C_{21}H_{20}ClN_4O_5^+$	443.1117	443.1114	−0.7	386	Human, monkey, rat	Confirmed by authentic standard	[16, 19]
MET34	Hydroxylated metabolite on the cyclopropyl moiety of lenvatinib	$C_{21}H_{20}ClN_4O_5^+$	443.1117	443.1116	−0.2	425, 387, 370, 344	Human, monkey, rat	Proposed	
MET35	Oxidated metabolite on the cyclopropylamine moiety of lenvatinib	$C_{21}H_{20}ClN_4O_5^+$	443.1117	443.1116	−0.2	370, 338	Rat	Proposed	
MET36	Oxidated metabolite on the cyclopropylamine moiety of M3’	$C_{21}H_{20}ClN_4O_6^+$	459.1066	459.1064	−0.4	424	Human	Proposed	
M2	Demethylated derivative of lenvatinib	$C_{20}H_{18}ClN_4O_4^+$	413.1011	413.1006	−1.2	396, 356, 330	Human, monkey, rat	Confirmed by authentic standard	[16, 19]
M3’	Quinolinone form of lenvatinib	$C_{21}H_{20}ClN_4O_5^+$	443.1117	443.111	−1.6	426, 386, 360, 343	Human, monkey	Confirmed by authentic standard	[19]
M2’	Quinolinone form of M2	$C_{20}H_{18}ClN_4O_5^+$	429.0960	429.0987	6.3	412, 372, 346, 355, 329	Human, monkey	Confirmed by authentic standard	[19]

Table 1 (continued)

Name	Description proposed identity	Formula	Calculated *m/z*	Observed *m/z*	Mass error (ppm)	Major fragment	Species	Structure characterization	Ref.*
MET41	Unknown	Unknown	Unknown	Unknown	NA	–	–		
MET42	2-mercaptoethanol conjugate of the demethylated quinoline moiety of lenvatinib	$C_{12}H_{12}N_2O_3S^+$	267.0674	267	NA	250, 222, 206	Human	Proposed	
MET43	2-mercaptoethanol conjugate of the quinoline moiety of lenvatinib	$C_{13}H_{14}N_2O_3S^+$	281.0830	281	NA	237, 220	Human	Proposed	

Ref: reference

* this metabolite was previously described in the referred paper(s)

identical to a MS^4 spectrum of 459) showed the following product ions: *m/z* 396 (additional loss of CO), *m/z* 388 (not assigned), *m/z* 353 (loss of oxidated cyclopropylamine) and *m/z* 327 (not assigned). The proposed identity of this metabolites is an oxidated metabolite on the cyclopropylamine moiety of M3'.

Metabolite M2

The identity of this metabolite was confirmed with the reference standard of M2: a demethylated derivative of lenvatinib). The MS-spectra and proposed fragmentation are included in Supplementary Figure 1. M2 had a protonated molecular ion at *m/z* 413.1006 and product ions at *m/z* 396.0738 (loss of NH_3), 356.0426 (loss of cyclopropylamine), 330.0637 (loss of cyclopropylformamide) and 313 (loss of cyclopropylformamide and NH_3). The MS^3 spectrum of *m/z* 396 showed a product ion at *m/z* 378 (additional loss of water).

Metabolite M3'

The identity of this metabolite was confirmed with the reference standard of M3': a quinolinone form of lenvatinib. The MS-spectra and proposed fragmentation are included in Supplementary Figure 1. M3' had a protonated molecular ion at *m/z* 443.1110 and product ions at *m/z* 426.0844 (loss of NH_3), *m/z* 386 (loss of cyclopropylamine), *m/z* 360.0740 (loss of cyclopropylformamide) and *m/z* 343.0474 (loss of cyclopropylurea). The MS^3 spectrum of *m/z* 426 showed product ions of *m/z* 409 (additional loss of 17 Da, not assigned), *m/z* 381 (additional loss of 45, not assigned), *m/z* 369 (additional loss of cyclopropylamine) and *m/z* 343 (additional loss of cyclopropylformide).

Metabolite M2'

The identity of this metabolite was confirmed with the reference standard of M2': a quinolinone form of demethylated lenvatinib. The MS-spectra and proposed fragmentation are included in Supplementary Figure 1. M2' had a protonated molecular ion at *m/z* 429.0987 and product ions at *m/z* 412.0691 (loss of NH_3), *m/z* 372.0378 (loss of cyclopropylamine), *m/z* 346.0585 (loss of cyclopropylformamide), *m/z* 355.0112 (loss of cyclopropylamine and NH_3) and *m/z* 329.0321 (loss of cyclopropylformamide and NH_3 or loss of cyclopropylurea). The MS^3 spectrum of *m/z* 412 showed product ions at *m/z* 395 (additional loss of 17 Da, not assigned), *m/z* 367 (additional loss of 45 Da, not assigned), *m/z* 355 (additional loss of cyclopropylamine) and *m/z* 329 (additional loss of cyclopropylformide). The MS^3 spectrum of *m/z* 329 (loss of cyclopropylformamide and NH_3 or loss of cyclopropylurea) showed product ions at *m/z* 301 (loss of cyclopropylformamide

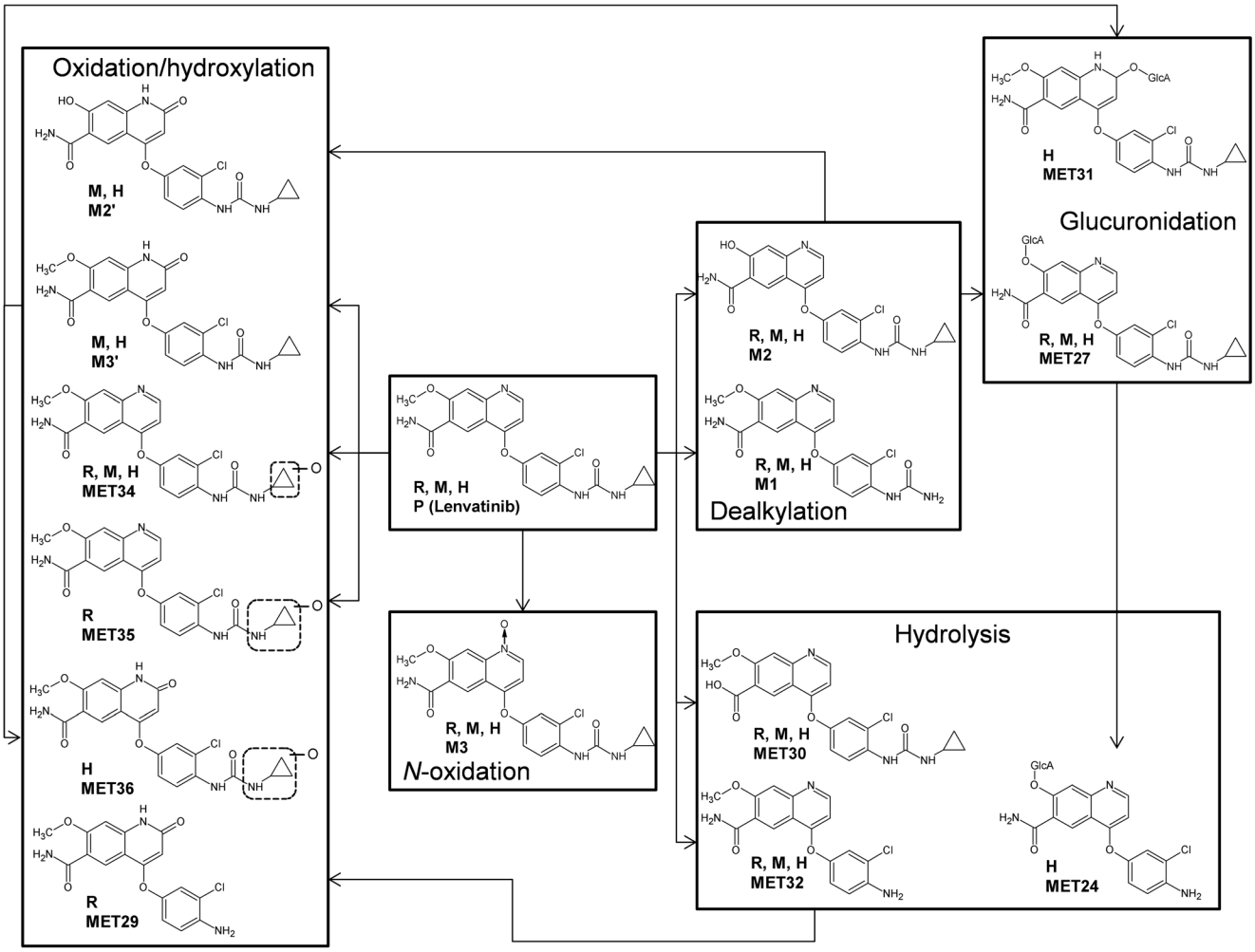

Fig. 6 Proposed metabolic scheme for lenvatinib in rat, monkey and human. R: metabolite found in rat sample(s); M: metabolite found in monkey sample(s); H: metabolite found in human sample(s)

and NH_3 and additional loss of CO), *m/z* 293 (additional loss of HCl), *m/z* 284 (loss of cyclopropylurea and additional loss of carboxamide group) and *m/z* 266 (loss of cyclopropylurea and additional loss of carboxamide group and water).

Unknown metabolites

As described above LC-MS^n was the primary tool to generate the profiles of the metabolites and to elucidate their molecular structures. This was performed by using a LC-LSC-MS setup in which peaks from the obtained radiochromatograms were compared to peaks in the MS chromatograms. In addition to the identified metabolites, there were peaks visible in the radiochromatograms that could not be matched to any peak in the MS chromatograms and were thus labeled unknown metabolites. These metabolites for which no molecular ion was identified and which were detected using chromatography method 1 were assigned a letter (A-E).

Metabolites A, B and D were found in human urine and accounted for 0.78, 0.99 and 3.7 %, respectively, of the administered ^{14}C-lenvatinib dose between 0 and 168 h after dosing. Metabolites C and E were found in human feces and accounted for 3.4 and 0.68 %, respectively, of the administered ^{14}C-lenvatinib dose between 0 and 168 h after dosing. None of these metabolites were detected in human plasma, so therefore no additional safety testing of drug metabolites is required according to the MIST guidelines [21].

Unknown metabolites detected using chromatographic method 2 were numbered according to their retention time (MET1, MET2, MET11, MET25 and MET41). Metabolites MET1, MET11 and MET25 were previously found in monkey plasma, rat urine and monkey bile, respectively. The structures of these metabolites were not elucidated and the metabolites were not detected in humans. Metabolites MET2 and MET41 were detected as an early (polar) and late (apolar) eluting peak in most matrices (see Fig. 5), but because no

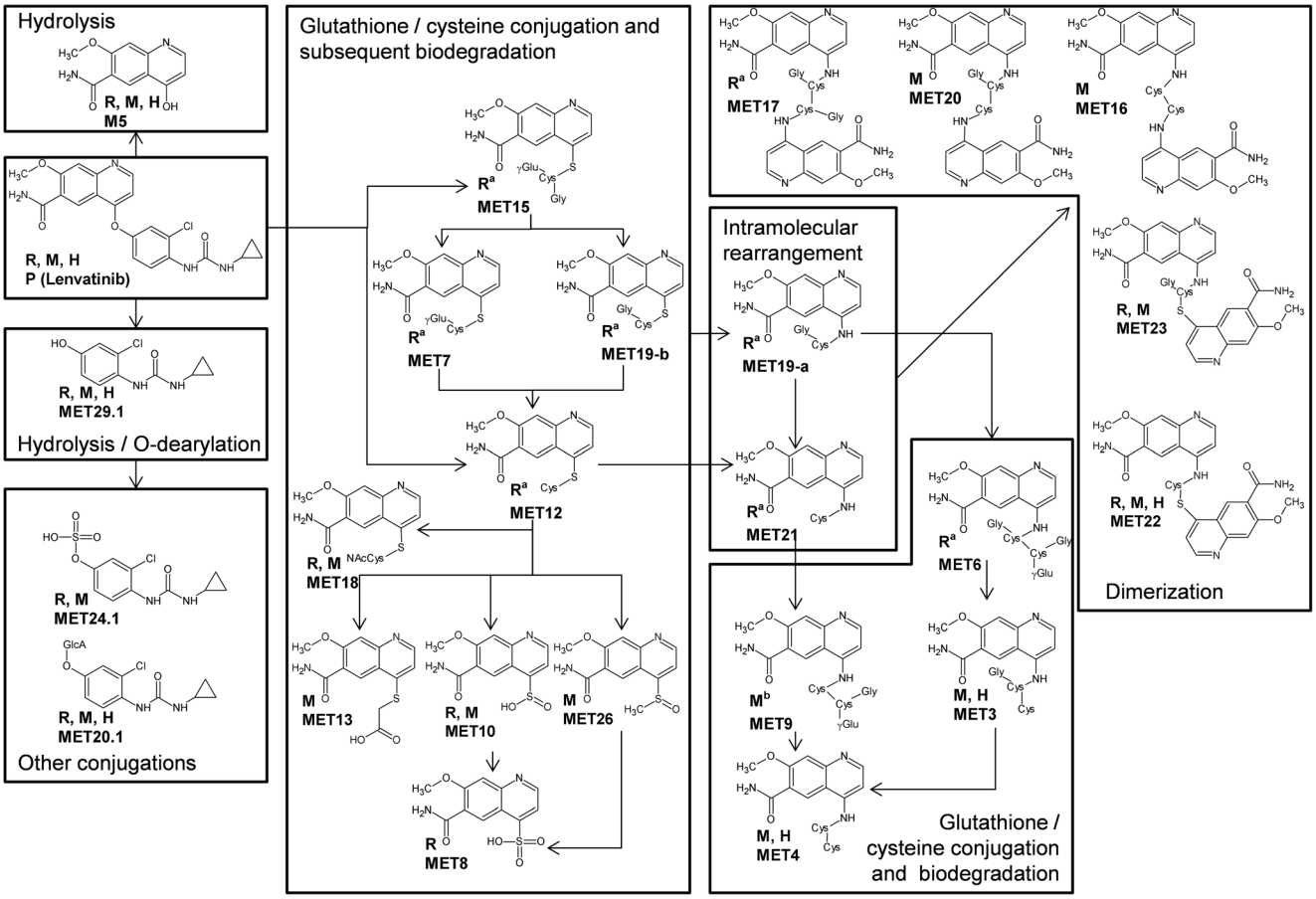

Fig. 7 Proposed metabolic scheme for lenvatinib in rat, monkey and human after splitting of lenvatinib in the quinolone and chlorophenol moieties. R: metabolite found in rat sample(s); R^a: metabolite only found in rat bile; M: metabolite found in monkey sample(s); M^b: metabolite only found in monkey liver (in a separate study); H: metabolite found in human sample(s)

molecular ion could be found also their identities remained unknown.

Discussion

This study aimed to determine the metabolism and disposition of lenvatinib in human and to elucidate the metabolic pathways of lenvatinib by investigating and comparing its metabolite profiles in rat, monkey and human samples after ^{14}C-lenvatinib administration. It was found that after administration of a single oral dose of ^{14}C-lenvatinib to 6 patients, 23 % of the radioactivity was recovered in urine and 65 % in feces collected over 168 h. The total recovery of 88 % found in this study corresponds with recovery of 89 % found in the previously published human mass balance study of ^{14}C-lenvatinib [16].

The chromatographic resolution of the radiochromatograms in this study is limited. The chromatographic separation could have been improved by using ultra high performance liquid chromatography (UHPLC) instead of HPLC and the chromatographic resolution in the radiochromatograms by collecting smaller fractions. However, because the measurement of radioactivity is based on absolute values, large injection volumes (up to 50 μL) needed to be injected onto the column in order to obtain detectable amounts of radioactivity in the fractions. These injection volumes are incompatible with UHPLC columns because of their small internal volume. Additionally, the fraction size of 1 min was selected to compromise between chromatographic resolution and sensitivity for the radioactivity measurements. Therefore the used methods were considered appropriate for the metabolite profiling of lenvatinib.

The preparation of plasma and feces for metabolite profiling suffered from low sample extraction recoveries. Various methods to increase the recovery were tested, such as increasing the organic solvent concentration in the reconstitution solution and varying the pH between 6.6 and 8.0 during the extraction. Although an increase in organic solvent concentration in the reconstitution solution did result in a higher recovery, a solvent effect was observed in the chromatography. An important difference was however observed between the two

matrices. During the sample preparation of plasma, compound-specific losses were suspected, because the extraction recovery decreased over collection time (Fig. 3a). A targeted analysis of non-radioactive lenvatinib-related compounds in selected plasma samples revealed that only MET29.1 could be detected. This suggests the presence of conjugates to the quinoline-moiety of lenvatinib that are covalently bound to plasma proteins, impeding their extraction. Because of their low abundancy, this could not be confirmed with the 2-ME treatment. Still, the unextracted radioactivity was therefore considered a separate group of metabolites and radiochromatographic peaks were not corrected for sample preparation recovery.

Contrary to the plasma samples, the feces samples showed no time-related trend in recovery (Fig. 3b), but they were observed to yield a higher extraction recovery in portions containing more water. The low sample preparation recovery was therefore most likely due to the inaccessible nature of the matrix, rather than due to the formation of non-extractable metabolites. This was supported by the treatment of the feces pellets after extraction with 2-ME. Instead of free thiol derivatives of the quinoline moiety of lenvatinib that were expected to be formed after 2-ME assisted reduction of disulfide bonds between these derivatives and proteins, only 2-ME conjugates of the quinoline moiety and demethylated quinoline moiety of lenvatinib were found (MET42 and MET43). Therefore, for feces, correction of radiochromatograms with the sample extraction recovery was considered acceptable.

Unchanged lenvatinib was the most predominant lenvatinib-related product in plasma. As opposed to the plasma samples, lenvatinib accounted for only a small amount of the radioactivity in urine (0.38 % of the administered dose) and feces (2.5 % of the administered dose). In this study around 50 compounds related to lenvatinib were detected in samples originating from rat, monkey and/or human. The majority of the chemical structures of these compounds were further characterized. The Proposed metabolic schemes of lenvatinib in rat, monkey and human are presented in Figs. 6 and 7.

Proposed phase 1 metabolic pathways of lenvatinib are (N-)oxidation, hydroxylation, dealkylation and hydrolysis. Some of the resulting metabolites were further metabolized, for example by conjugation with glucuronic acid, sulphate or glutathione. Figure 6 gives an overview of these metabolic pathways. *N*-oxidation of lenvatinib resulted in M3. Oxidation or hydroxylation at the cyclopropyl moiety resulted in formation of MET34 and MET35. In line with a previously reported oxidative metabolic pathway of lenvatinib (Inoue et al., 2014), also oxidation products in the form of a quinolinone were detected. These were M3', which can directly be formed from lenvatinib by aldehyde oxidase [19], MET36, which is proposed to be a product of oxidation of M3', M2', which can only be formed via the demethylated lenvatinib metabolite (M2) [19] and MET29, which is proposed to be formed from the product of lenvatinib hydrolysis of the cyclopropylformamide moiety (MET32). A second hydrolysis product, whereby the amine group is hydrolyzed, is assigned MET30. A second dealkylation product is M1, the decyclopropylated form of lenvatinib.

Glucuronic acid conjugation of M2 and M3' resulted in formation of MET27 and MET31, respectively. Hydrolysis of the cyclopropylformamide moiety of MET27 resulted in the formation of MET24.

An additional metabolic pathway of lenvatinib is proposed in Fig. 7. Lenvatinib is proposed to be hydrolytically split into the quinoline moiety M5 and the non-radiolabeled chlorophenol moiety MET29.1. The chlorophenol moiety of lenvatinib was conjugated with sulphate, resulting in MET24.1 and with glucuronic acid, resulting in MET20.1.

As was demonstrated by Inoue et al. [15], the chlorophenol moiety of lenvatinib could also be displaced by either glutathione, to form MET15, or by cysteine, to form an S-linked cysteine conjugate of the quinoline moiety MET12. The latter (MET12) could also be formed from biodegradation of the glutathione conjugate (MET15), after formation of a γ-glutamyl-cysteine conjugate (MET7) or an S-linked cysteinylglycine conjugate (MET19b) of the quinoline moiety of lenvatinib.

Also biodegradation products of the S-linked cysteine conjugate of the quinoline moiety (MET12) were observed, whereby the cysteine conjugate was proposed to be transformed to N-acetylcysteine (mercapturic acid) (resulting in MET18), mercaptoacetic acid (resulting in MET13), sulphinic acid (resulting in MET10), methyl sulphoxide (resulting in MET26) or sulphonic acid (resulting in MET8, [22]). This metabolic pathway generally follows the glutathione biodegradation pathway as reported by Levsen et al. [23].

Also N-linked cysteine (MET21) and cysteinylglycine (MET19a) conjugates of the quinoline moiety were observed. These were probably formed by intramolecular S-to-N rearrangement of (MET12) and (MET19a), respectively, as previously described by Inoue et al. [15]. The N-linked cysteine (MET21) and cysteinylglycine (MET19a) conjugates were in turn conjugated with glutathione, resulting in MET9 (only observed in monkey liver, not in present study) and MET6, respectively. Degradation products of cysteine (MET4) and cysteinylglycine (MET3) adducts of the quinoline moiety of lenvatinib were detected, too. Finally, homo- and hetero dimers of the N-linked cysteine (MET21) and cysteinylglycine (MET19a) conjugates were observed, whereby two quinoline moieties were bound by cysteine (MET22), cysteinylglycine (MET23), cysteine (MET16), cysteinylglycine and cysteine (MET20) or two cysteinylglycine groups (MET17).

In summary, the biotransformation of lenvatinib is very extensive in the three investigated species. The primary pathways for biotransformation of lenvatinib were hydrolysis,

oxidation and hydroxylation, N-oxidation, dealkylation and glucuronidation. These results confirm the preclinical results that were published previously [15, 19]. The great majority of the proposed lenvatinib metabolites described in this study, has never been described before. Some metabolic pathways seem to be unique for different species. Pathways that are unique for rats and monkey are gluthathione and cysteine conjugation of lenvatinib only and the subsequent rearrangement was only seen in rats. Dimerization of metabolites was more common in monkey and rat samples. In humans MET22 was the only found dimerized metabolite. MET36, MET31 and MET24 were only detected in human samples and MET3, MET4, M3' and M2' were only detected in human and monkey samples. In general, the formation of quinolinone derivatives of lenvatinib was far more common in human than in monkey and rat. This variability in metabolite presence in different species makes it difficult to compare potential toxicity issues with lenvatinib and metabolites between these species. It is however known that some quinolinone metabolites of other drugs can crystallize which may cause species-specific renal toxicity [24]. Nevertheless, the low levels of metabolites found in human plasma as compared to unchanged lenvatinib suggest a limited contribution of metabolites to the toxicity of lenvatinib. Additionally, because of their minor presence in human plasma, the metabolites are not expected to contribute to the efficacy seen with the compound.

Acknowledgments The authors would like to thank the patients who gave their valuable time to participate in the human mass balance study.

Authorship contributions

Participated in research design: Dubbelman, Jansen, Mizuo, Critchley, Shumaker, Nijenhuis, Rosing

Conducted experiments: Dubbelman, Jansen, Nijenhuis

Performed data analysis: Dubbelman, Nijenhuis

Wrote or contributed to the writing of the manuscript: Dubbelman, Jansen, Mizuo, Kawaguchi, Nijenhuis, Rosing, Schellens, Beijnen

Compliance with ethical standards

Conflict of interest Hitoshi Mizuo and Shinki Kawaguchi are employees of Eisai Co. Ltd., David Critchley is an employee of Eisai Ltd. and Robert Shumaker in an employee of Eisai Inc. All other authors declare no conflict of interest.

References

1. Tohyama O, Matsui J, Kodama K, Hata-Sugi N, Kimura T, Okamoto K, Minoshima Y, Iwata M, Funahashi Y (2014) Antitumor activity of lenvatinib (e7080): an angiogenesis inhibitor that targets multiple receptor tyrosine kinases in preclinical human thyroid cancer models. J Thyroid Res 2014:638747. doi:10.1155/2014/638747
2. Yamamoto Y, Matsui J, Matsushima T, Obaishi H, Miyazaki K, Nakamura K, Tohyama O, Semba T, Yamaguchi A, Hoshi SS, Mimura F, Haneda T, Fukuda Y, Kamata J, Takahashi K, Matsukura M, Wakabayashi T, Asada M, Nomoto K, Watanabe T, Dezso Z, Yoshimatsu K, Funahashi Y, Tsuruoka A (2014) Lenvatinib, an angiogenesis inhibitor targeting VEGFR/FGFR, shows broad antitumor activity in human tumor xenograft models associated with microvessel density and pericyte coverage. Vasc Cell 6:18. doi:10.1186/2045-824X-6-18
3. Matsui J, Funahashi Y, Uenaka T, Watanabe T, Tsuruoka A, Asada M (2008) Multi-kinase inhibitor E7080 suppresses lymph node and lung metastases of human mammary breast tumor MDA-MB-231 via inhibition of vascular endothelial growth factor-receptor (VEGF-R) 2 and VEGF-R3 kinase. Clin Cancer Res 14(17):5459–5465. doi:10.1158/1078-0432.CCR-07-5270
4. Matsui J, Yamamoto Y, Funahashi Y, Tsuruoka A, Watanabe T, Wakabayashi T, Uenaka T, Asada M (2008) E7080, a novel inhibitor that targets multiple kinases, has potent antitumor activities against stem cell factor producing human small cell lung cancer H146, based on angiogenesis inhibition. Int J Cancer 122(3):664–671. doi:10.1002/ijc.23131
5. Okamoto K, Kodama K, Takase K, Sugi NH, Yamamoto Y, Iwata M, Tsuruoka A (2013) Antitumor activities of the targeted multi-tyrosine kinase inhibitor lenvatinib (E7080) against RET gene fusion-driven tumor models. Cancer Lett 340(1):97–103. doi:10.1016/j.canlet.2013.07.007
6. Cabanillas ME, Schlumberger M, Jarzab B, Martins RG, Pacini F, Robinson B, McCaffrey JC, Shah MH, Bodenner DL, Topliss D, Andresen C, O'Brien JP, Ren M, Funahashi Y, Allison R, Elisei R, Newbold K, Licitra LF, Sherman SI, Ball DW (2015) A phase 2 trial of lenvatinib (E7080) in advanced, progressive, radioiodine-refractory, differentiated thyroid cancer: a clinical outcomes and biomarker assessment. Cancer 121(16):2749–2756. doi:10.1002/cncr.29395
7. Hong DS, Kurzrock R, Falchook GS, Andresen C, Kwak J, Ren M, Xu L, George GC, Kim KB, Nguyen LM, O'Brien JP, Nemunaitis J (2015) Phase 1b study of lenvatinib (E7080) in combination with temozolomide for treatment of advanced melanoma. Oncotarget 6(40):43127–43134. doi:10.18632/oncotarget.5756
8. Hong DS, Kurzrock R, Wheler JJ, Naing A, Falchook GS, Fu S, Kim KB, Davies MA, Nguyen LM, George GC, Xu L, Shumaker R, Ren M, Mink J, Bedell C, Andresen C, Sachdev P, O'Brien JP, Nemunaitis J (2015) Phase I dose-escalation study of the multikinase inhibitor lenvatinib in patients with advanced solid tumors and in an expanded cohort of patients with melanoma. Clin Cancer Res 21(21):4801–4810. doi:10.1158/1078-0432.CCR-14-3063
9. Ikeda M, Okusaka T, Mitsunaga S, Uneo H, Tamai T, Suzuki T, Hayato S, Kadowaki T, Okita K, Kumada H (2015) Safety and pharmacokinetics of lenvatinib in patients with advanced hepatocellular carcinoma. Clin Cancer Res. doi:10.1158/1078-0432.CCR-15-1354
10. Molina AM, Hutson TE, Larkin J, Gold AM, Wood K, Carter D, Motzer R, Michaelson MD (2014) A phase 1b clinical trial of the multi-targeted tyrosine kinase inhibitor lenvatinib (E7080) in combination with everolimus for treatment of metastatic renal cell carcinoma (RCC). Cancer Chemother Pharmacol 73(1):181–189. doi:10.1007/s00280-013-2339-y
11. Motzer RJ, Hutson TE, Glen H, Michaelson MD, Molina A, Eisen T, Jassem J, Zolnierek J, Maroto JP, Mellado B, Melichar B, Tomasek J, Kremer A, Kim HJ, Wood K, Dutcus C, Larkin J (2015) Lenvatinib, everolimus, and the combination in patients with metastatic renal cell carcinoma: a randomised, phase 2, open-label, multicentre trial. Lancet Oncol 16(15):1473–1482. doi:10.1016/S1470-2045(15)00290-9

12. Nishio M, Horai T, Horiike A, Nokihara H, Yamamoto N, Takahashi T, Murakami H, Yamamoto N, Koizumi F, Nishio K, Yusa W, Koyama N, Tamura T (2013) Phase 1 study of lenvatinib combined with carboplatin and paclitaxel in patients with non-small-cell lung cancer. Br J Cancer 109(3):538–544. doi:10.1038/bjc.2013.374
13. Schlumberger M, Tahara M, Wirth LJ, Robinson B, Brose MS, Elisei R, Habra MA, Newbold K, Shah MH, Hoff AO, Gianoukakis AG, Kiyota N, Taylor MH, Kim SB, Krzyzanowska MK, Dutcus CE, de las Heras B, Zhu J, Sherman SI (2015) Lenvatinib versus placebo in radioiodine-refractory thyroid cancer. N Engl J Med 372(7):621–630. doi:10.1056/NEJMoa1406470
14. Mayor S (2015) Lenvatinib improves survival in refractory thyroid cancer. Lancet Oncol 16(3):e110. doi:10.1016/S1470-2045(15)70066-5
15. Inoue K, Asai N, Mizuo H, Fukuda K, Kusano K, Yoshimura T (2012) Unique metabolic pathway of [(14)C]lenvatinib after oral administration to male cynomolgus monkey. Drug Metab Dispos 40(4):662–670. doi:10.1124/dmd.111.043281
16. Dubbelman AC, Rosing H, Nijenhuis C, Huitema AD, Mergui-Roelvink M, Gupta A, Verbel D, Thompson G, Shumaker R, Schellens JH, Beijnen JH (2015) Pharmacokinetics and excretion of (14)C-lenvatinib in patients with advanced solid tumors or lymphomas. Invest New Drugs 33(1):233–240. doi:10.1007/s10637-014-0181-7
17. Zhu M, Zhao W, Vazquez N, Mitroka JG (2005) Analysis of low level radioactive metabolites in biological fluids using high-performance liquid chromatography with microplate scintillation counting: method validation and application. J Pharm Biomed Anal 39(1–2):233–245. doi:10.1016/j.jpba.2005.03.012
18. Dubbelman AC, Rosing H, Schellens JH, Beijnen JH (2011) Bioanalytical aspects of clinical mass balance studies in oncology. Bioanalysis 3(23):2637–2655. doi:10.4155/bio.11.276
19. Inoue K, Mizuo H, Kawaguchi S, Fukuda K, Kusano K, Yoshimura T (2014) Oxidative metabolic pathway of lenvatinib mediated by aldehyde oxidase. Drug Metab Dispos. doi:10.1124/dmd.114.058073
20. Dubbelman AC, Rosing H, Thijssen B, Gebretensae A, Lucas L, Chen H, Shumaker R, Schellens JH, Beijnen JH (2012) Development and validation of LC-MS/MS assays for the quantification of E7080 and metabolites in various human biological matrices. J Chromatogr B Analyt Technol Biomed Life Sci 887–888:25–34. doi:10.1016/j.jchromb.2012.01.004
21. US Food and Drug Administration (2008) Guidance for industry: safety testing of drug metabolites, US Department of Health and Human Services, Food and Drug Administration, Center for Drug Evaluation and Research http://www.fda.gov/OHRMS/DOCKETS/98fr/FDA-2008-D-0065-GDL.pdf. Accessed at: 06-01-2016
22. Pretsch E, Bühlmann P, Affolter C (2013) Structure determination of organic compounds: tables of spectral data. Mass Spectrometry, 3rd edn. Springer Science & Business Media
23. Levsen K, Schiebel HM, Behnke B, Dotzer R, Dreher W, Elend M, Thiele H (2005) Structure elucidation of phase II metabolites by tandem mass spectrometry: an overview. J Chromatogr A 1067(1–2):55–72
24. Diamond S, Boer J, Maduskuie TP Jr, Falahatpisheh N, Li Y, Yeleswaram S (2010) Species-specific metabolism of SGX523 by aldehyde oxidase and the toxicological implications. Drug Metab Dispos 38(8):1277–1285. doi:10.1124/dmd.110.032375